enthalpy of the flow is to be increased by heating the shock tunnel driver section.

References

[1] Ball, H. W., "Calibration of the 100-inch Hypervelocity Tunnel F," AEDC-TDR-63-46 (AD298279), March 1963, Arnold Engineering Development Center, Arnold Air Force Station, Tenn.

[2] Griffith, B. J. and Weddington, E. D., "Recent Refinements and Advancements of Hypersonic Testing Techniques in the 100-inch Tunnel F of the von Kármán Gas Dynamics Facility," *Proceedings of the Fourth Hypervelocity Techniques Symposium*, Arnold Engineering Development Center, Arnold Air Force Station, Tenn., Nov. 15–16, 1965.

[3] Osgerby, I. T. and Smithson, H. K., "Operation of AEDC-VKF 100-inch Hotshot Tunnel F with Air as a Test Gas and Application to SCRAMjet Testing," AEDC-TR-67-242 (AD-664906), Dec. 1967, Arnold Engineering Development Center, Arnold Air Force Station, Tenn.; also presented at the Fifth Hypervelocity Techniques Symposium, Univ. of Denver, Colo., March 1967.

[4] Ball, H. W., "Initial Operation of the Pilot Counterflow Test Unit (I)," AEDC-TR-65-132 (AD465893), July 1965, Arnold Engineering Development Center, Arnold Air Force Station, Tenn.

[5] Haun, J. H. and Ball, H. W., "Calibration of the Shock Tunnel Component of Counterflow Range (I) at Mach 7.5," AEDC-TR-66-64 (AD632816), May 1966, Arnold Engineering Development Center, Arnold Air Force Station, Tenn.

[6] Hilsenrath, J. and Klein, M., "Tables of Thermodynamic Properties of Air in Chemical Equilibrium Including Second Virial Corrections from 1500°K to 15,000°K," AEDC-TR-65-68 (AD612301), March 1965, Arnold Engineering Development Center, Arnold Air Force Station, Tenn.

[7] Grabau, M. and Brahinsky, H. S., "Thermodynamic Properties of Air from 300 to 6000°K and from 1 to 1000 Amagats," AEDC-TR-66-247 (AD646172), Jan. 1967, Arnold Engineering Development Center, Arnold Air Force Station, Tenn.

[8] Lewis, C. H. and Burgess, E. G., III, "Charts of Normal Shock Wave Properties in Imperfect Air," AEDC-TDR-64-43 (AD433958), March 1964, Arnold Engineering Development Center, Arnold Air Force Station, Tenn.

[9] Pergament, H. S., "A Theoretical Analysis of Non-Equilibrium Hydrogen-Air Reactions in Flow Systems," AIAA, Paper 63-113, White Oak, Md., 1963.

[10] Whitfield, J. D. and Norfleet, G. D., "Source Flow Effects in Conical Hypervelocity Nozzles," AEDC-TDR-62-116 (AD276124), June 1962, Arnold Engineering Development Center, Arnold Air Force Station, Tenn.

[11] Arthur, P. D. et al., "Flat Plate Turbulent Heat Transfer at Hypervelocities," *Journal of Spacecraft and Rockets*, Vol. 3, No. 10, Oct. 1966, pp. 1549–1551.

[12] Osgerby, I. T., Smithson, H. K., and Wagner, D. A., "Development of a Double-Oblique-Shock SCRAMjet Model in a Shock Tunnel," AEDC-TR-69-59, Aug. 1969, Arnold Engineering Development Center, Arnold Air Force Station, Tenn.

APRIL 1971 J. AIRCRAFT VOL. 8, NO. 4

Transonic Flight and Wind-Tunnel Buffet Onset Investigation of the F-8D Aircraft

E. K. Damstrom* and J. F. Mayes†
LTV Aerospace Corporation, Dallas, Texas

Flight and wind-tunnel tests of the F-8D aircraft were conducted within Mach 0.72 to 0.92 to establish the proper interpretation of various wind-tunnel data in predicting flight buffet onset. The divergence of the root-mean-square wing bending moment fluctuation agreed best with the flight onset defined by $\pm 0.05g$ peak-to-peak fluctuation of normal acceleration at the center of gravity. Buffet onset trimmed lift coefficient was increased approximately 0.08 when $\pm 0.05g$ normal acceleration fluctuation at the pilot station, rather than center of gravity, was used to define flight onset. The flight test data analysis disclosed an interesting decrease of the predominant frequency of acceleration fluctuation with increasing trimmed lift coefficient during the maneuver. Analysis of flight data suggested that the g level, as well as frequency and amplitude of g fluctuation, should be considered if buffet intensity is to be related to pilot functional capability.

Nomenclature

$\bar{c}$	= wing mean geometric chord, excluding leading-edge chord extension (141.4 in., full scale)
$c.g._{flt}$	= flight center-of-gravity location, fraction of $\bar{c}$
$c.g._{wt}$	= wind-tunnel moment reference location, fraction of $\bar{c}$
C_A	= axial force coefficient, axial force/$(q_\infty S)$
C_L	= lift force coefficient, lift/$(q_\infty S)$
C_m	= pitching moment coefficient, pitching moment/$(q_\infty S\bar{c})$ (ref. about $0.286\bar{c}$)
C_p	= wing trailing-edge pressure coefficient, $(P - P_\infty)/(q_\infty S)$
g	= gravitational acceleration unit
N_Y	= lateral acceleration, g
N_Z	= normal acceleration, g
P	= wing trailing-edge static pressure, lb/ft^2
P_∞	= freestream static pressure, lb/ft^2
q_∞	= freestream dynamic pressure, lb/ft^2
RN/L	= freestream unit Reynolds number, ft^{-1}
S	= reference area, wing area excluding leading-edge chord extension (375 ft^2, full scale)
x/c	= chordwise station measured from leading edge of wing, including leading-edge chord extension, fraction of chord
$y/(b/2)$	= spanwise station measured from plane of symmetry, fraction of semispan
α	= angle of attack of fuselage, deg

Presented as Paper 70-341 at the AIAA Fighter Aircraft Conference, St. Louis, Mo., March 5–7, 1970; submitted April 6, 1970; revision received July 24, 1970. The authors wish to acknowledge the contribution of the wind-tunnel data by NASA and the valuable assistance of E. J. Ray of NASA and H. R. Barnard of LTV Aerospace Corporation.

* Engineering Specialist, External Aerodynamics Group, Vought Aeronautics. Member AIAA.

† Senior Engineer, External Aerodynamics Group, Vought Aeronautics. Member AIAA.

ΔN = peak-to-peak fluctuation of acceleration N, g
σ_{rms} = rms wing bending moment fluctuation, in.-lb

Subscripts

c.g. = flight center of gravity
L = lower surface
OFF = horizontal tail off
ON = horizontal tail on
PS = pilot station
TRIM = trimmed
U = upper surface

I Introduction

INCREASED attention is being given to studies of buffet characteristics to meet the design requirements for future aircraft. Because of the complexity of the buffet problem it is not easily amenable to theoretical solution. Therefore, most previous investigations have involved wind-tunnel tests to predict buffet onset and to provide some indication of buffet intensity. The most recent and best controlled wind-tunnel investigation to determine the effect of wing geometric parameters such as aspect ratio, sweep, thickness ratio, maximum thickness position, and camber is described by Ray and Taylor.[1] Perhaps Pearcey[2] presents the most complete coverage of the buffet problem. Until recent years, the classical approach throughout industry was to use the divergence of C_L vs α as the buffet onset criterion. However, the stringent maneuverability requirements of future aircraft in the high subsonic regime near Mach 1.0 dictate an improved definition of the buffet characteristics which will occur during flight. As a result, considerable emphasis is now placed on obtaining the various types of wind-tunnel data which provide a more reliable indication of boundary-layer separation on the wing surface of sufficient magnitude to cause buffet. Present wind-tunnel testing techniques, therefore, include strain-gage measurements of wing bending moment fluctuation, static pressure measurements along the wing trailing edge, and flow visualization, such as oil flow photographs, in addition to the usual force and pitching moment measurements. (These wind-tunnel measurements have been treated by Mayes, et al.[3])

An understanding of the relationships between the various types of wind-tunnel data is helpful in the interpretation of the data with regard to flow separation on the wind-tunnel model. Since flow separation is the source of buffet, wind-tunnel data alone are sufficient to establish if a change in wing design is favorable from a buffet standpoint. The application, however, of the wind-tunnel data to a flight aircraft requires some means of accounting for the effects of flight Reynolds number and airframe structural dynamics, effects which cannot be simulated adequately during a wind-tunnel test. In the absence of a suitable technique for establishing these effects, both flight and wind-tunnel tests of the F-8D aircraft were conducted so that data from these tests could be used as a basis for future predictions. The flight test program involved measurements of normal acceleration at the c.g. and both normal and lateral acceleration at the pilot station.

The LTV flight and NASA-Langley wind-tunnel test programs for the F-8D aircraft are presented in the following sections. The instrumentation required to obtain usable data is discussed and the analysis of these data and test techniques are presented.

II Flight Test

The No. 1 F-8D (Bu. No. 147035) was used to obtain the flight buffet data. The primary objective of the test was to measure the small peak-to-peak acceleration fluctuations sensed by the pilot, so that the buffet onset lift coefficient for $\pm 0.05g$ peak-to-peak fluctuation of normal acceleration at the c.g. or pilot station could be established. Additional objectives of the flight test were a) to assess the effect of fuselage flexibility on the normal acceleration fluctuations at the pilot station, as compared to the fluctuations at the c.g., and b) to investigate the dependence of the predominant frequency of normal acceleration fluctuation on the normal g level, or trimmed lift, in the buffet region. Lateral acceleration measurements at the pilot station provided additional data for buffet analysis. The data were obtained with no leading-edge droop (undeflected leading-edge flaps), and with no stores or pylons. Wing fuel tanks were empty so that there would be no influence of wing fuel dynamics on the buffet results. The basic wing geometry is presented in Table 1.

Instrumentation

A block diagram of the flight test instrumentation used to obtain acceleration measurements is shown in Fig. 1. Identical instrumentation, except for the accelerometer g range, was chosen to measure the acceleration at the two locations so that a high degree of confidence could be placed on results obtained by comparing the data for the two locations. The requirement of detecting small fluctuations was satisfied by using servo force balance accelerometers having a natural frequency of approximately 200 cps and a flat frequency response of 0 to 100 cps. It was desirable to use accelerometers having a low g-range capability to achieve a high degree of accuracy.

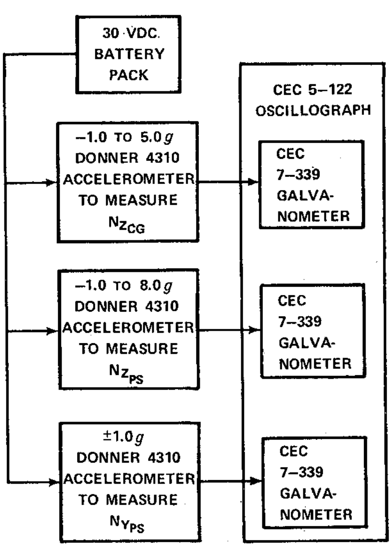

Fig. 1 Flight test instrumentation.

Table 1 Wing geometry

Geometric parameter[a]	Full scale value
Area	375 ft²
Span	35.67 ft
Tip chord	49.93 in.
Root chord	202.0 in.
Mean geometric chord	
length	141.4 in.
spanwise location from plane of symmetry	85.6 in.
Taper ratio	0.247
Aspect ratio	3.4
Quarter-chord sweep	42.0°
Incidence relative to fuselage reference line	−1.0°
Anhedral	5.0°
Geometric twist	0.0°
Airfoil sections, parallel to fuselage plane of symmetry, at	
butt line = 20 in.	NACA 65A006
wing tip	NACA 65A005

[a] Excludes 12% leading-edge chord extension outboard of 63% semispan location.

Although the available accelerometers were not identical in this respect, the departure from a common g range was not considered sufficient to prohibit comparison of the accelerometer measurements, especially the normal acceleration at the c.g. and pilot station. A -1 to $+5g$ range accelerometer was mounted on the aft landing gear bulkhead to measure the normal acceleration at the c.g. Even though this location (0.52 $\bar{c}$) was somewhat aft of the actual c.g. location (0.23 to 0.25 $\bar{c}$) during flight, the accelerometer measurements should be representative of the acceleration at the c.g. The normal and lateral accelerations at the pilot station were measured by a -1 to $+8g$ and a $\pm 1g$ range accelerometer, respectively, mounted on the left back rail of the pilot seat.

The detection of small acceleration fluctuations also demanded special provisions with regard to transducer mounting, electrical excitation, and recording sensitivity. In order that mounting bracket resonant frequencies would be 500 cps or greater, rigid mounting was used. Electrical excitation for the accelerometers was supplied by a 30 VDC battery pack so that power fluctuation effects would be eliminated. An oscillograph located in the ammo compartment recorded the accelerometer measurements at a paper speed of six in./sec so that all frequencies recorded could be detected. The oscillograph used galvanometers having a natural frequency of 50 cps (critically damped) and a flat frequency response of 0 to 30 cps. The trace deflections on the photosensitive oscillograph paper were chosen to give the highest recording sensitivity of approximately $1g$ normal acceleration and $0.4g$ lateral acceleration per in.

Test Conditions and Results

Flight-test data were obtained at pressure altitudes of approximately 28,000 and 36,000 ft, and at Mach numbers from 0.72 to 0.92. Three types of maneuvers (windup turns, wings-level pullups, and steady-g turns) were performed to determine any effect of the type of maneuver on the results. Wings-level pushovers were also performed to obtain data near zero lift. The variable-g maneuvers were performed at a slow rate of approximately $0.10g$/sec to assure no effect of pitch rate on the results and to provide a sufficient time history for proper analysis. During each maneuver, the pilot indicated by an "event" signal recorded on the oscillograph paper the time at which he first sensed buffet as the g level increased.

The flight data were reduced by measuring the peak-to-peak g fluctuation (ΔN) on the oscillograph trace at various points during the maneuver. During the data reduction, care was taken to account for the trace width, which could erroneously have been taken to represent approximately $0.02g$ normal acceleration or $0.01g$ lateral acceleration. Acceleration time histories before pilot threshold of buffet, after pilot threshold of buffet, and at maximum normal acceleration during a left windup turn are reproduced in Fig. 2. The acceleration fluctuations for the variable-g maneuvers were reduced at a sufficient number of points to define the ΔN variation during the maneuver. The normal g levels necessary to determine the lift coefficient were established by taking a point within the fluctuating trace which would be representative of the mean acceleration. The product of the airplane weight and the normal g level at the c.g. was used to define the lift force. Previous F-8 flight data indicated that the trimmed lift coefficient established in this manner for these maneuvers is, in general, within 1% of a more accurate computation by summing the components of normal acceleration, longitudinal acceleration, and engine thrust in the lift direction. This negligible computation inaccuracy was verified by comparing the wind-tunnel measurements of lift and normal force coefficients discussed in Sec. III.

The normal acceleration fluctuations for the steady-g maneuvers were reduced at the beginning, the middle, and the end of each maneuver, which lasted approximately 10 sec, to obtain a check of repeatability. These data were obtained at Mach numbers of approximately 0.75 and 0.90. No check of repeatability at a given trimmed lift coefficient could be made in the data analysis because of the data scatter. This data scatter is attributed primarily, if not entirely, to the varying flight conditions which the pilot could not maintain constant during the maneuver.

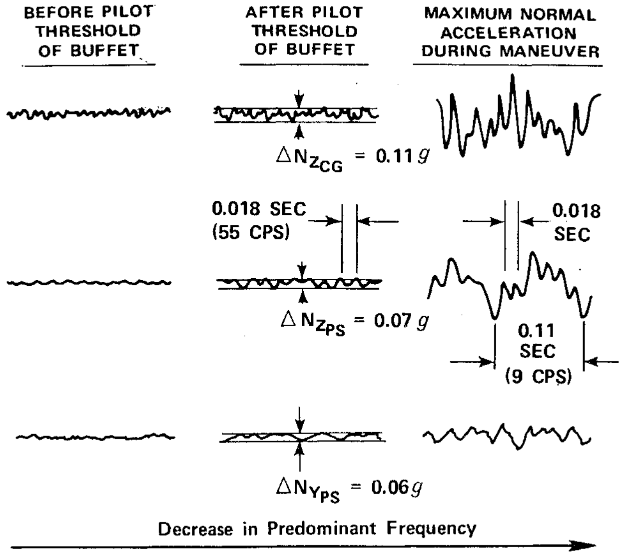

Fig. 2 Acceleration time histories for typical maneuver.

Variable-throttle steady-g turns at low g levels were also performed to confirm the absence of engine rpm effects on the buffet results. Measurements of aileron position and sideslip angle revealed that these parameters seldom exceeded $\pm 1.0°$ and never exceeded $\pm 2.0°$ during these maneuvers.

III Wind-Tunnel Test

A 0.042 scale rigid model of the F-8D aircraft with no leading-edge droop (symmetrical wing airfoil sections), and with no stores or pylons was tested in the 7 $\times$ 10 ft high-speed tunnel at NASA-Langley to obtain buffet data for comparison with the flight data. The wind-tunnel data included measurements of wing bending moment fluctuation and trailing-edge pressure as well as the usual force and moment data.

Instrumentation

A six-component balance was used to measure aerodynamic forces and pitching moment, and the right wing of the model was instrumented to obtain wing bending moment fluctuation and trailing-edge pressure data. The strain-gage installation to measure wing bending moment fluctuation and the pressure orifice locations are shown in Fig. 3. A temperature-compensated strain-gage bridge (four foil gages, two upper and two lower) was oriented along the 50% chord line, the approximate location of the elastic axis, to minimize any torsional effects as nearly as practical. A schematic drawing of the instrumentation associated with the strain-gage measurements is shown in Fig. 4. Upper and lower surface pressure orifices were installed at seven spanwise stations near the trailing edge, as shown in Fig. 3, to define the extent of boundary-layer separation associated with buffet. It was desirable to install all orifices as near as possible to the trailing edge, in this case at the 95–96% chord station, including leading-edge chord extension. However, the thinness of the wing near the tip prevented fabrication of the most outboard orifice on both upper and lower surface any farther aft than the 88% chord station.

A transition strip of number 80 grit was used at the 40% chord location on the wing, and number 120 grit was placed

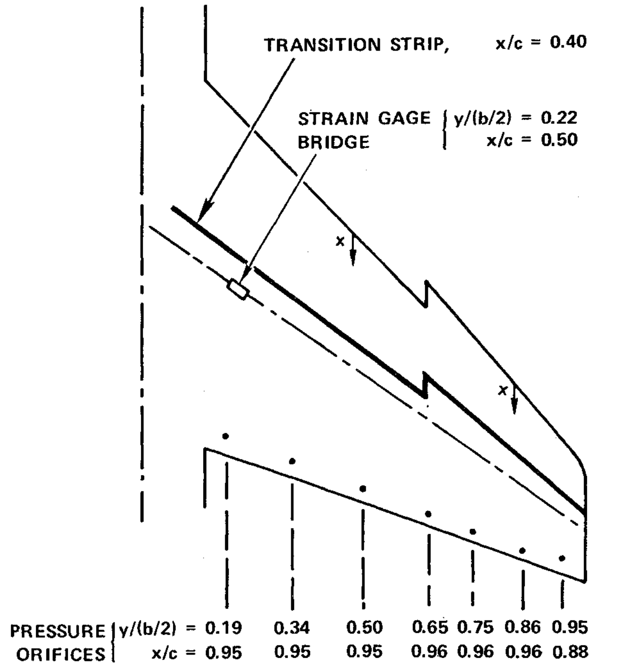

Fig. 3 Strain gage and pressure orifice installation on wind-tunnel model.

0.5 in. aft of the nose of the body and the leading edge of all other model components.

Test Conditions and Results

Wind-tunnel data were taken at Mach numbers covering the range of 0.75 to 0.92 and at a Reynolds number of approximately 3.5 million/ft. The original plan was to obtain all types of data simultaneously so that the various data would be for exactly the same test conditions for analysis purposes. This was not achieved, however, because the necessary clearance between the model and sting required for valid force and pitching moment data was partially filled with the trailing-edge pressure tubing extending out of the model base. The test procedure, therefore, was first to obtain trailing-edge pressure and wing bending-moment fluctuation data and then to make additional runs to measure aerodynamic forces and pitching moment. Strain-gage measurements of wing bending-moment fluctuation were also obtained during these additional runs to supplement the strain-gage data obtained during the pressure measurements and to provide a check on the repeatability. The previous runs were made with the horizontal tail off. Selected runs were also made with the horizontal tail at -5 and $-10°$ deflection (trailing edge up) to measure forces, pitching moment, and wing bending moment fluctuations. Axial force was corrected for freestream pressure at the model base by using the measured cavity pressure. Each data value for the wing bending-moment fluctuation represented the rms value over a 45-sec time interval.

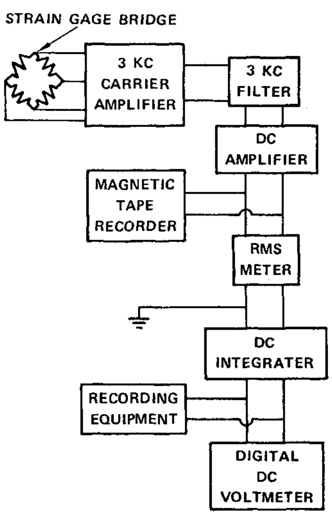

Fig. 4 Wind-tunnel strain gage instrumentation.

IV Flight—Wind-Tunnel Analysis

Buffet boundaries were established by a detailed analysis of the flight and wind-tunnel data. Buffet onset during flight was determined for two criteria based on the normal acceleration fluctuations at the c.g. and pilot station. Because of the data scatter for the steady-g turns, analysis was confined to the data for the windup turns and wings-level pullups to establish buffet onset. The wind-tunnel buffet onset was determined primarily from the measurements of the wing bending-moment fluctuation.

Flight Data Analysis

The first step in the analysis of the flight data was to select a peak-to-peak value of normal acceleration to define buffet onset. This was achieved by comparing the acceleration amplitude ($0.5\ \Delta N_{ZPS}$) at pilot perception of buffet with vibration data given by Harris and Crede[4] for various subjects in standing, sitting and lying positions. This comparison, presented in Fig. 5, shows that, in general, the F-8D data agree with the threshold-of-perception region and are below the unpleasant region established by the vibration data. An acceleration amplitude between these two regions was believed to be a realistic representation of buffet onset; therefore, a normal acceleration fluctuation of $\pm 0.05g$ near the upper limit of the F-8D data was chosen to define buffet onset.

The procedure to establish the flight boundary made no distinction of the acceleration sources. Though it is acknowledged that engine vibrations, for example, exist, and indeed may have been detected to a minor extent by the accelerometers, a satisfactory method of distinguishing between these acceleration sources and wing pressure fluctuations due to flow separation is not presently accessible. Also, the pilot's opinion of tolerable or intolerable vibrations is independent of the vibration source. Therefore, to avoid any misleading conclusions which may arise by attempting to isolate the various acceleration sources, the procedure to establish the flight boundary included all acceleration sources in the buffet onset definition of $\pm 0.05g$ normal acceleration; i.e., onset was established for $\Delta N_{Zc.g.} = 0.10g$ and for $\Delta N_{ZPS} = 0.10g$.

The variation of the g fluctuation with angle of attack was subject to two interpretations, as shown in Fig. 6 for a typical maneuver. One approach was to draw a curve (dashed in the

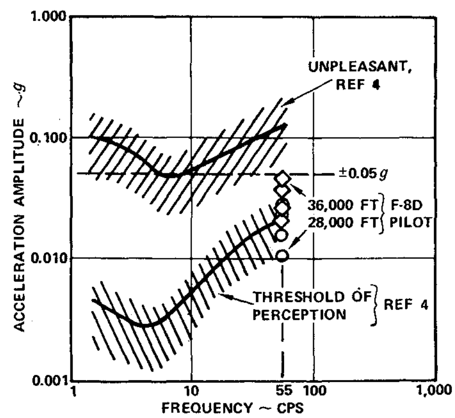

Fig. 5 Acceleration tolerance criteria.

figure) through the data points. Another approach was to fair a curve (solid line) through the points, considering an accuracy of approximately 10% in data reduction for values of ΔN_Z in the neighborhood of $0.10g$. The trimmed lift coefficient using these two interpretations is shown in Fig. 7 for the criteria, $\Delta N_{Z\text{c.g.}} = 0.10g$ and $\Delta N_{ZPS} = 0.10g$. Any difference in the result obtained by the two interpretations is indicated in the figure by the spread attached to the symbol. The hump in the boundary near Mach 0.75 is similar to boundaries for onset of separation effects presented by Pearcey.[2] In this reference Pearcey associates the low Mach number side of this region of the boundary with the transition from leading-edge to shock-induced separation as Mach number is increased.

The data points in Fig. 7 indicate no apparent effect of altitude on the buffet boundary when one considers the data scatter. The plotted data, however, do show that onset may be dependent on the type of maneuver, as indicated by the lower values of onset $C_{L\text{TRIM}}$ for the pull-ups. An important result to be gained from these data is the higher buffet boundary when the $\pm 0.05g$ fluctuation at the pilot station, rather than c.g., is used to define onset. This $C_{L\text{TRIM}}$ difference of approximately 0.08 is attributed to the relieving effect of the fuselage due to structural flexibility. A qualitative analysis of the acceleration traces for the F-105F airplane given by Williams[5] also revealed a fuselage attenuation between c.g. and pilot station.

One purpose of the flight-test program was to determine the relative magnitudes of the normal and lateral fluctuations at the pilot station. The data showed that ΔN_{YPS} was approximately equal to or somewhat less than ΔN_{ZPS}, e.g., see Fig. 2.

The three acceleration traces revealed a dependence of fluctuation frequency on normal g level, or trimmed C_L. For example, the normal acceleration at the pilot station fluctuated at approximately 55 cps near pilot perception of buffet and continued to fluctuate at this frequency up to the maximum g level (maximum trimmed C_L) during the maneuver, as illustrated in Fig. 2. However, as the g level was increasing, a lower frequency of approximately 9 cps occurred and appeared to become the predominant frequency at maximum C_L. This frequency trend, confirmed by the pilot, is characteristic of the flight data (wing tip acceleration and wing bending moment fluctuations) for the F-105F given by Williams[5] and the low-speed wind-tunnel pressure fluctuation data for the Bristol 188 obtained by Lawford and Beauchamp.[6]

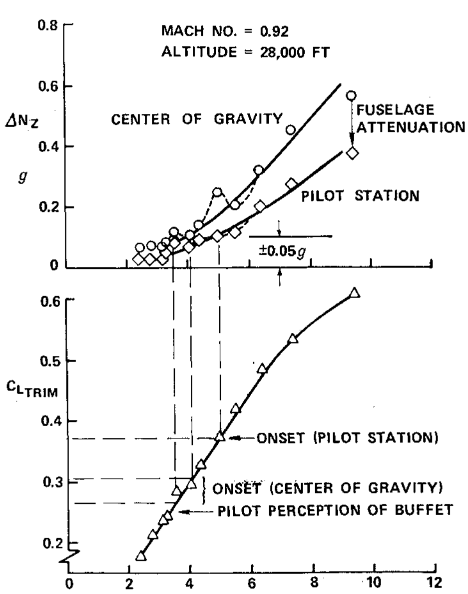

Fig. 6 Determination of flight buffet onset for $\pm 0.05g$ normal acceleration fluctuation.

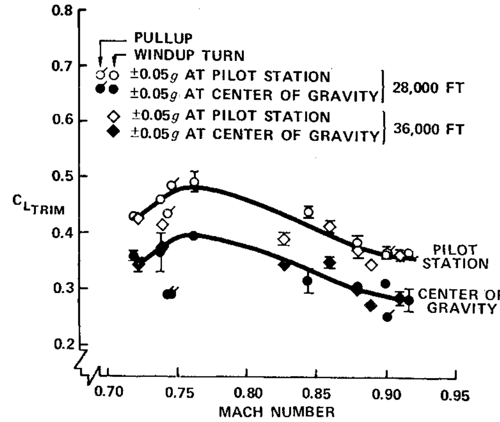

Fig. 7 Flight buffet onset boundary for $\pm 0.05g$ normal acceleration fluctuation.

These more irregular acceleration fluctuations at the higher normal g levels made it difficult to determine a representative peak-to-peak value for $\Delta N_{Z\text{c.g.}}$, ΔN_{ZPS}, and ΔN_{YPS}; therefore, the value at the higher normal g levels (higher angles of attack) may be in error as much as $\pm 50\%$. The error at the lower g levels near pilot perception of buffet is, in general, believed to be nearer $\pm 10\%$.

As a matter of interest, it is appropriate to mention that a visual analysis of the oscillograph traces of the flight measurements for the F-105F indicates that the frequency of local wing-pressure fluctuations is very nearly identical to the frequency of the wing bending moment and the normal acceleration at the wing tip. The absence of this high frequency of approximately 70 cps on the oscillograph traces for the normal acceleration at the c.g. and pilot station of the F-105F may be due to the use of galvanometers having a flat frequency response up to only approximately 12 cps for measuring the acceleration at these two locations. Since a high frequency (55 cps) of normal acceleration fluctuation occurred at the F-8D pilot station, it is speculated that there may be some predictable relation between the frequency and amplitude of local pressure fluctuation and the frequency and amplitude of normal acceleration fluctuation which is sensed by the pilot.

Wind-Tunnel Data Analysis

The trailing-edge pressure data were analyzed by first plotting the variation of both upper and lower pressure with angle of attack on the same plot, as shown for Mach 0.75 in Fig. 8a. These pressure data show the upper surface pressure to decrease at the faster rate, as might be expected because of the proximity of the upper orifice to the region of flow separation. Observation of this difference between upper and lower trailing-edge pressure and a desire to eliminate any misleading effects of boundary layer growth led to a further analysis of the pressure data. This involved a plot of the variation of the difference between upper and lower trailing-edge pressure, also shown in Fig. 8a.

Although some pressure orifices were inoperative, the pressure data were analyzed in more detail to investigate the spanwise extent of boundary-layer separation associated with buffet. In this analysis, separation of sufficient magnitude to cause buffet was taken to be the divergence of the upper trailing-edge pressure, the lower pressure, or the upper-minus-lower pressure differential. Since these three parameters are characterized in most cases by a gradual decrease from a nearly constant value, the divergence point was established by extrapolating the nearly constant value and the nearly linear variation, as illustrated for C_{PU} in Fig. 8a. The spanwise variations of the angle of attack corresponding to the divergence of upper and lower trailing-edge pressure are shown in Fig. 8b to be very similar. The spanwise variation obtained by using the upper-minus-lower pressure differential

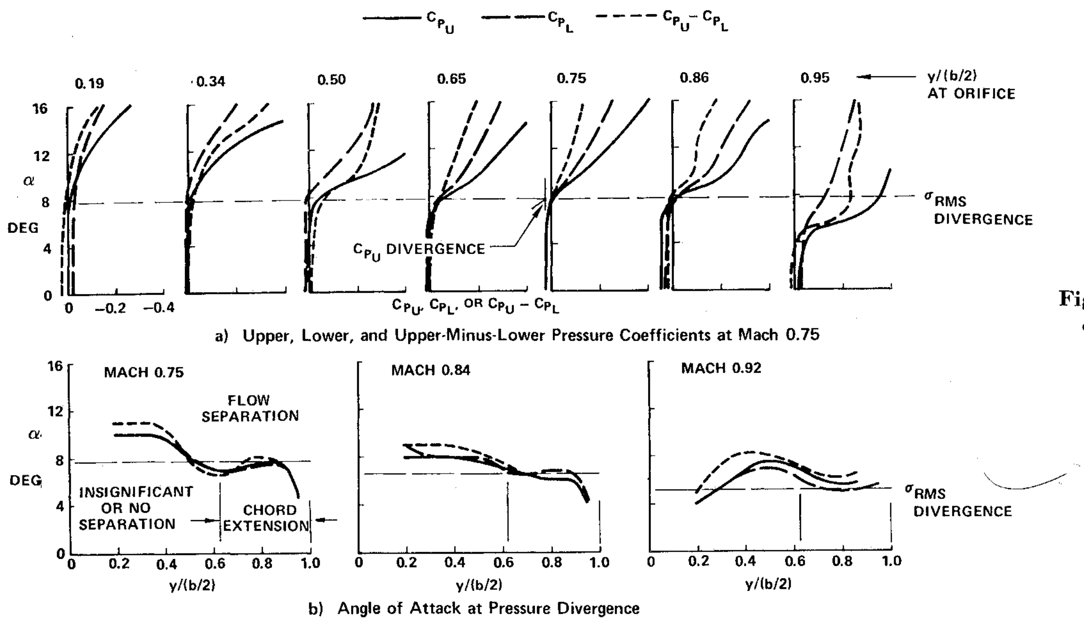

Fig. 8 Wing trailing-edge pressure data.

generally indicates slightly higher values. All three plots, however, indicate that at the lower Mach numbers, boundary-layer separation first occurred near the wing tip. At Mach 0.92, fuselage-wing interference or a stronger, more normal shock system in the inboard region may have caused the early divergence at the most inboard orifice. The unfavorable slope of the curves just inboard of the 63% semispan location does not continue farther outboard because of the favorable vortex system that originates at the leading-edge break introduced by the chord extension.

The divergence of the trailing-edge pressure coefficient plotted vs Mach number at a given angle of attack should also be examined in a buffet onset analysis. As pointed out by Pearcey and Holder,[7] the lower of the two points determined by using trailing-edge pressure coefficient vs both angle of attack and Mach number should be used to define buffet onset based on trailing-edge pressure. The trailing-edge pressure values at the various Mach numbers for a particular orifice indicated no lower value of angle of attack for the divergence of C_P vs Mach number than the value for divergence of C_P vs angle of attack. Therefore, the conservative divergence points in Fig. 8b represent the final result of analyzing both divergences of C_P.

A special composite plot of the various wind-tunnel data facilitated analysis and interpretation. This composite plot used to establish the wind-tunnel buffet onset boundary is shown in Fig. 9. The curves showing the variation of wing bending-moment fluctuation were established from all rms measurements taken at the three Mach numbers at which force data were obtained. The initial level of the rms curve increased with Mach number, consistent with the results which were obtained by Ray and Taylor[1] in the same wind tunnel. This initial level is due to nonboundary-layer-separation effects such as wind-tunnel turbulence. Buffet onset was established primarily by the point of divergence of the rms curve from the nearly constant level. This point (illustrated at Mach 0.75 in Fig. 9) occurs within the nearly linear variation of lift coefficient vs angle of attack and to

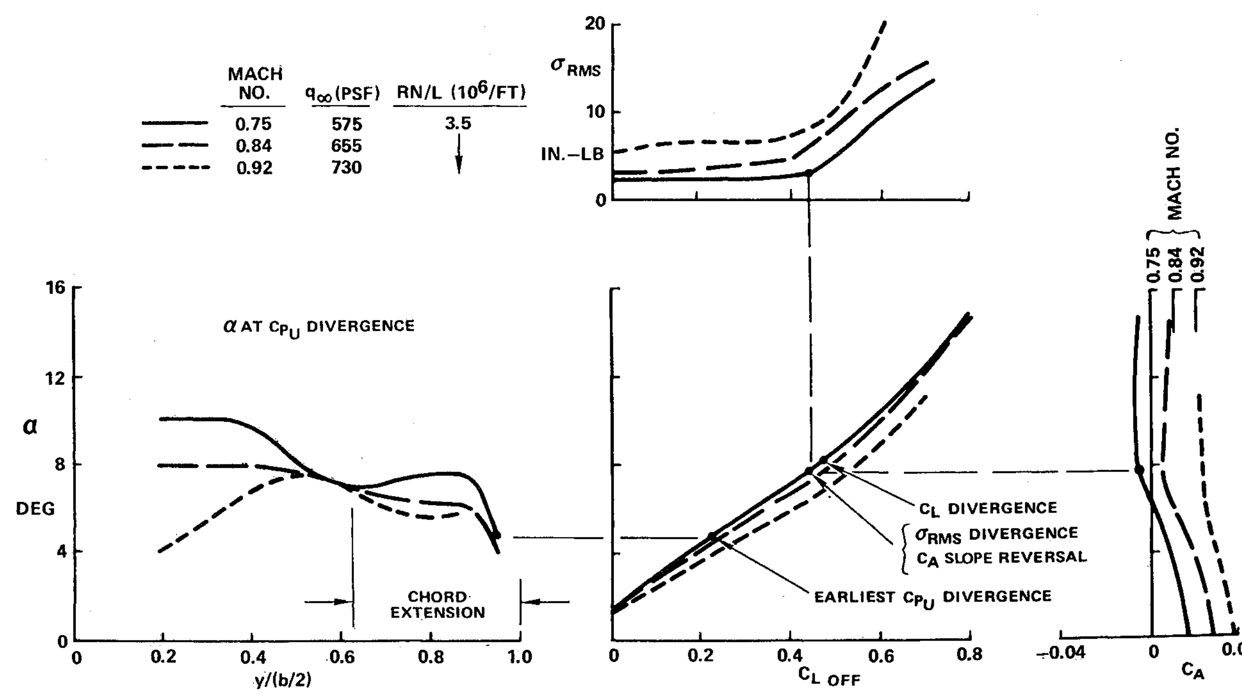

Fig. 9 Composite of wind-tunnel buffet onset data.

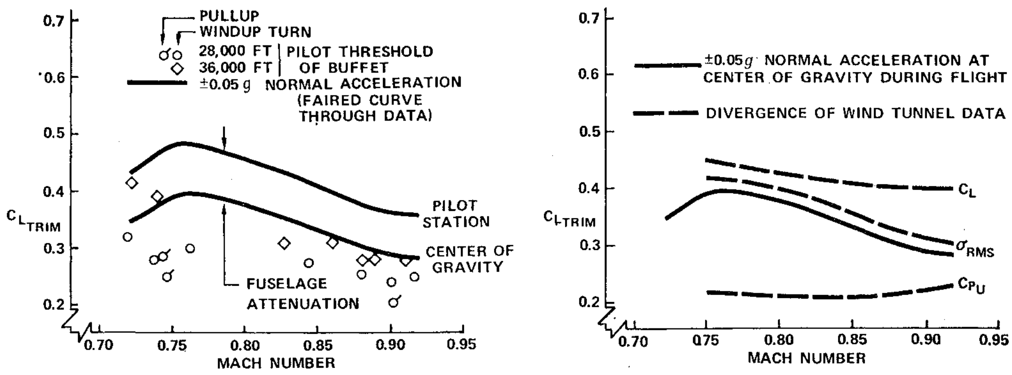

a) Flight

b) Flight – Wind Tunnel Comparison

Fig. 10 Summary of buffet onset boundaries.

agree closely with the reversal in slope of axial force coefficient. This is in accord with the general relationship between the variation of wing bending moment and axial force data of Ray and Taylor[1] at these Mach numbers.

A necessary step of the wind-tunnel data analysis was to determine the trimmed lift coefficient at buffet onset, so that the results could be compared with the flight-test data. The trimmed lift coefficient was first established by simply using the horizontal-tail-off force and moment data in computing the trim lift, the aerodynamic center defined by the quarter chord point on the mean geometric chord of the horizontal tail extended to the plane of symmetry. A check of this procedure for determining the trimmed lift throughout the Mach number range was provided by using the tail-on data, obtained at Mach 0.75 and 0.92, as well as the tail-off data in the following equation:

$$C_{L\mathrm{TRIM}_{c.g.}} = C_{L\mathrm{OFF}} \left[\frac{\left(\dfrac{C_{m\mathrm{ON}} - C_{m\mathrm{OFF}}}{C_{L\mathrm{ON}} - C_{L\mathrm{OFF}}}\right) - \dfrac{C_{m\mathrm{OFF}}}{C_{L\mathrm{OFF}}}}{\left(\dfrac{C_{m\mathrm{ON}} - C_{m\mathrm{OFF}}}{C_{L\mathrm{ON}} - C_{L\mathrm{OFF}}}\right) + \mathrm{c.g.}_{\mathrm{flt}} - \mathrm{c.g.}_{\mathrm{wt}}} \right]$$

The lift coefficient obtained by using data for both tail deflections, -5 and $-10°$, in this more precise expression justified the simpler computations to determine the final trimmed lift coefficient at all three Mach numbers.

The wing bending-moment fluctuation data may have provided an indication of the repeatability of the rms values of the wing bending-moment fluctuation. The presence of the horizontal tail is thought to have a small effect on the strain-gage measurements. Kemp and King[8] concluded that the strain-gage data for the D-558-II airplane was not significantly influenced by tail buffeting. However, the measurements at the highest Mach number are suspected of being significantly influenced by wind-tunnel turbulence and the somewhat periodic nature of maximum model-sting shaking which was observed to occur at all angles of attack and to be more pronounced at the highest Mach number. It seems likely that in future analysis of wind-tunnel measurements the repeatability of the rms moment fluctuation may perhaps be improved if the effect of model-sting shaking is eliminated by a power-spectral-density analysis of the fluctuation measurements.

Flight—Wind-Tunnel Comparison

The main purpose of the flight and wind-tunnel tests was to gain a better understanding of the relation between buffet onset established from wind-tunnel measurements and onset which will occur during the flight of future aircraft. The approach chosen to fulfill this need was to compare the flight and wind-tunnel onset boundaries for the F-8D aircraft and then, at some future date, to examine similar results for other operational aircraft.

The buffet results of the F-8D flight and wind-tunnel tests are summarized in Fig. 10. The data points for the pilot threshold of buffet in Fig. 10a are shown, in most cases, to be below the boundaries defined by $\pm 0.05g$ normal acceleration. The undesirable data scatter indicate that total reliance on pilot opinion to establish a criterion for the flight buffet onset boundary would not be satisfactory. A measurable quantity, such as $\pm 0.05g$ normal acceleration, based to some extent on pilot opinion is believed to be a more meaningful criterion.

The wind-tunnel onset boundary based on wing bending moment fluctuation is shown in Fig. 10b to be similar to the flight boundaries based on normal acceleration fluctuation. The wind-tunnel onset $C_{L\mathrm{TRIM}}$ is only 0.02 higher than the flight boundary corresponding to $\pm 0.05g$ normal acceleration at the c.g. In fact, the wind-tunnel boundary is within the scatter of the flight data based on c.g. acceleration presented in Fig. 7. This close agreement is not too surprising, because the strain-gage bridge sensed the wing bending-moment fluctuation very near the wing root of the model and the accelerometer at the c.g. of the flight aircraft detected the fluctuating wing aerodynamic forces which were transmitted directly to a region of the fuselage near the c.g. location. The wind-tunnel onset $C_{L\mathrm{TRIM}}$ is approximately 0.06 lower than the flight boundary in Fig. 10a corresponding to $\pm 0.05g$ normal acceleration at the pilot station. As mentioned previously in this section, the higher boundary for the $\pm 0.05g$ criterion at the pilot station is ascribed to the relieving effect of the fuselage due to structural flexibility between the c.g. and pilot station. The flight and wind-tunnel data suggest that the divergence of wind-tunnel rms measurements of wing bending-moment fluctuation corresponds very closely to a $\pm 0.05g$ peak-to-peak normal acceleration fluctuation at the c.g.

The wind-tunnel boundaries based solely on the earliest divergence of trailing-edge pressure (illustrated at Mach 0.75 in Fig. 9) or lift coefficient are shown in Fig. 10b to depart significantly from the flight boundary based on normal acceleration at the c.g. At the lower Mach numbers the earlier divergence of the trailing-edge pressure occurred because of flow separation near the wing tip (see Figs. 8 and 9) which was not detected by either the flight accelerometer or by the wind-tunnel strain-gage measurements. The better agreement at the higher Mach numbers is due to a tendency toward a more uniform spanwise distribution of incipient flow separation, as shown in Figs. 8 and 9. The less accurate boundary defined by the more gradual divergence of lift coefficient is shown to be too optimistic, especially at the higher Mach numbers.

The pilot-opinion data scatter in Fig. 10a prompted further analysis. The lower pilot onset points in this figure occurred at the lower altitude, and the lower amplitude of g fluctuation at pilot threshold of perception in Fig. 5 also occurred at the lower altitude. It is realized that in order to fly at the same Mach number and lift coefficient at a lower altitude, a higher g level is required because of a higher dynamic pressure, i.e., a higher inertia force must balance the higher lift force at the lower altitude. These observations suggested the possible dependence of pilot perception of vibration on the g level as well as amplitude and frequency of g fluctuation. Analysis of both the g level and fluctuation amplitude at the pilot station when the pilot first sensed buffet indicated, in general, that at or near the same Mach number a lower amplitude at the lower altitude was associated with a higher g level than that experienced by the pilot at the higher altitude. Since even a nonfluctuating acceleration is objectionable from a human-factors standpoint when the acceleration is too high, an explanation for the lower amplitude at the lower altitude (higher g level) and also the pilot-opinion scatter in Fig. 10a, might be that a given amplitude of fluctuation is "magnified" —from the standpoint of buffet intensity as sensed by the pilot—by an increase in g level. This may suggest that the g level, as well as frequency and amplitude of g fluctuation, should be considered if buffet intensity is to be related to a pilot's ability to perform his tasks in the buffet region.

V Conclusions and Recommendations

The foregoing analysis of flight and wind-tunnel data resulted in a number of conclusions reached within the scope of the various test measurements of this paper. The following conclusions are believed to be applicable to fighter-type aircraft which exhibit wing structural response characteristics similar to the F-8D.

1) The divergence of the wind-tunnel rms measurements of wing bending moment fluctuation corresponds closely to the flight boundary for a $\pm 0.05g$ peak-to-peak normal acceleration fluctuation at the c.g. The wind-tunnel onset boundary determined to predict flight buffet onset should, it seems, depend primarily on the divergence of wing bending-moment fluctuation, provided no significant separation occurs inboard of the strain-gage bridge.

2) Pilot opinion alone is not satisfactory as a criterion for the flight onset boundary because of data scatter. Some magnitude of a measurable quantity, such as a peak-to-peak normal acceleration of $\pm 0.05g$, established to some extent by pilot perception and tolerance of vibrations is believed to be a more meaningful criterion.

3) There is a neglibible effect, if any, of altitude variation from 28,000 to 36,000 ft on the buffet boundary based on $\pm 0.05g$ normal acceleration.

4) During a constant-Mach-number flight maneuver such as a windup turn, the predominant frequency of acceleration fluctuation is expected to decrease with increasing normal g level, or trimmed lift coefficient. It is speculated that there may be some predictable relation between the frequency and amplitude of local pressure fluctuations and the frequency and amplitude of normal acceleration fluctuation which is sensed by the pilot.

5) The normal g level, as well as the frequency and amplitude of g fluctuation, should perhaps be considered if buffet intensity is to be related to pilot functional capability.

An important flight result pertinent to only F-8 aircraft is an increase, due to fuselage attenuation, in buffet-onset trimmed-lift coefficient of approximately 0.08 when a $\pm 0.05g$ fluctuation at the pilot station, rather than c.g., is used to define onset. Wind-tunnel results revealed that the reversal in the slope of axial force vs angle of attack occurs very near the divergence of the wing bending-moment fluctuation. However, the earliest divergence of trailing-edge pressure at some spanwise location, usually near the wing tip, occurs much earlier at the lowest Mach number (0.75), and the divergence of lift coefficient occurs much later at the highest Mach number (0.92).

Consideration of identical types of flight and wind-tunnel measurements, taken simultaneously during the flight or wind-tunnel test, is recommended to gain additional knowledge toward improving buffet onset predictions and accounting for structural dynamics effects. In addition to wing bending-moment fluctuation and trailing-edge pressure, the following types of data should perhaps be obtained during both flight and wind-tunnel tests: upper-surface pressure fluctuations and boundary-layer surveys, flow visualization photos, wing-tip normal acceleration fluctuations, and wing torsional moment fluctuations. Flight data may also include aileron hinge moment fluctuation and the fluctuation of all three acceleration components at various locations on the aircraft. Fluctuating wake pressure measurements may be acquired during a wind-tunnel test. It is recommended that all flight and wind-tunnel fluctuation measurements be recorded on magnetic tape to permit a power-spectral-density analysis and the determination of an rms value which may be a better definition of buffet onset. Future flight tests might include flights at low as well as high altitude to establish the effect of normal g level on a pilot's opinion of buffet intensity as well as perception of buffet.

VI References

[1] Ray, E. J. and Taylor, R. T., "Buffet and Static Aerodynamic Characteristics of a Systematic Series of Wings Determined from a Subsonic Wind-Tunnel Study," TN D-5805, June 1970, NASA.

[2] Lachmann, G. V., ed., *Boundary Layer and Flow Control*, 1st ed., Vol. 2, Pergamon, New York, 1961, pp. 1166–1344.

[3] Mayes, J. F., Lores, M. E., and Barnard, H. R., "Transonic Buffet Characteristics of a 60° Swept Wing with Design Variations," *Journal of Aircraft*, Vol. 7, No. 6, Nov.–Dec. 1970, pp. 524–530.

[4] Harris, C. M. and Crede, C. E., eds., *Shock and Vibration Handbook*, 1st ed., Vol. 3, McGraw-Hill, New York, 1961, Chap. 44, p. 40.

[5] Williams, D., "Buffet Boundary," Eng. Flight Rept. 274, Aug. 1968, Fairchild Hiller, Republic Aviation Division, Farmingdale, N. Y.

[6] Lawford, J. A. and Beauchamp, A. R., "Low Speed Wind Tunnel Measurements of Pressure Fluctuations on the Wing of a Twin Jet Aircraft (Bristol 188)," TR 66399, Dec. 1966, Royal Aircraft Establishment, Farnborough Hants, Great Britain.

[7] Pearcey, H. H. and Holder, D. W., "Simple Methods for the Prediction of Wing Buffeting Resulting from Bubble-Type Separation," Aero Rept. 1024, June 1962, National Physical Laboratory, Teddington, Great Britain.

[8] Kemp, W. B., Jr. and King, T. J., "Wind Tunnel Measurements of Wing Buffeting on 1/16-Scale Model of Douglas D-558-II Research Airplane," RM L56G31, Sept. 1956, NASA.